JCHR (2017) 7(4), 285-298

Journal of Chemical Health Risks

www.jchr.org

ORIGINAL ARTICLE

Preparation of SBA-15-PAMAM as a Nano Adsorbent for Removal of Acid Red 266 from Aqueous Media: Batch Adsorption and Equilibrium Studies

Maryam Mirzaie[1], Abosaeed Rashidi[1], Habib-Allah Tayebi*[2], Mohammad Esmail Yazdanshenas[3]

[1]Department of Textile Engineering, Science and Research Branch, Islamic Azad University, Tehran, Iran

[2]Department of Textile Engineering, Qaemshahr Branch, Islamic Azad University, Qaemshahr, Iran

[3]Department of Textile Engineering, Yazd Branch, Islamic Azad University, Yazd, Iran

(Received: 17 May 2017 Accepted: 7 July 2017)

KEYWORDS

Dye removal;
BA-15-Den;
Adsorption;
Isotherm;
Langmuir;

ABSTRACT: The purpose of the present study was to increase the adsorption capacity of SBA-15 for acidic dyes. Ordered mesoporous silica SBA-15 was successfully synthesized and functionalized by polyamidoamine (PAMAM) dendrimer to develop an efficient anionic dye adsorbent. The prepared materials were characterized by field emission scanning electron microscope (FE-SEM), Fourier transforms infrared spectroscope (FT-IR) and N_2 adsorption–desorption analysis. The study was concocted in the Science and Research Branch of Islamic Azad University of Tehran, Iran in 2016. The produced adsorbent (SBA-15-Den) was applied for the removal of Acid Red 266 (AR266) from aqueous media. The effects of various operational parameters including solution pH, adsorbent dosage, contact time, and temperature on removal of AR266 using SBA-15-Den were investigated in batch adsorption mode. Within the optimum conditions, SBA-15-Den exhibited an excellent adsorptive capability of 1111.11 mg/g. Equilibrium data were best described by Langmuir model ($R^2 > 0.98$) completely.

INTRODUCTION

During the past years, several chemical and physical methods have been used to remove the dye from the aqueous media, which changing in operating cost, usefulness and environmental effect [1, 2]. Adsorption of dye molecules on the adsorbent can be a very appropriate and low-cost process for dye removal from aqueous media [3, 4]. Adsorption has been applied particularly for the removal of organic compounds from aqueous media [5]. SBA-15 meso structured silica was initiated, which includes of parallel cylindrical pores with axes ordered in a hexagonal unit cell [6].

* Corresponding author: tayebi_h@yahoo.com (H. Tayebi).

Commonly, SBA-15 with pores ranging from 5 to 30 nm has wider pores than MCM-41 and superior pore volume. Besides, as compared with other meso structured silica materials, SBA-15 has thicker pore walls between 3.1 and 6.4 nm, which supply high hydrothermal stability [6, 7], and is appropriate for applying in aqueous solutions. Mesoporous silica material SBA-15 has appealed considerable consideration since its discovery [8, 9]. The mesoporous silica materials, with well-behaved stability, have been applied in different fields such as separation and adsorption [10], catalysis [11], enzyme immobilization [12], its particular morphology is significant in various designed usage [13]. The SBA-15 is new Nano porous silica with high surface area, hexagonal construction, wide pore size, broad pore wall thickness, and high thermal resistance [14]. Dendrimers suggest major chances in molecular design due to their multifunctional characteristics such as host-guest chemistry, dendritic catalysts, medical application, etc. [15]. In our procedure for chemical modification of SBA-15, a dendrimer is one of the attractive molecules because of its multi functionality. Dendrimers are converting more introduced as nanomaterial stabilizers or covering agents. Therefore, it is because they have high loading valence due to their Nano hollows. In dendrimers, the nanoparticles might be shaped either in the internal hollows or in the perimeter of the dendrimers. Normally the nanoparticles' preparation within the dendrimers comprises two procedures [16-17].

The purpose of the present study was to increase the adsorption capacity of SBA-15 for acidic dyes. To carry out this idea, SBA-15 is properly modified by grafting of 3-chloropropyl trimethoxysilane as the anionic quality. The SBA-15-Den has not been considerably studied for the removal of acidic dyes. The operating convertibles such as pH, time contact, adsorbent dosage and temperature of the process were selected to consider the adsorption capacity of SBA-15-Den. The Langmuir, Freundlich, Temkin and Dubbin Radushkevich isotherms were applied to coordinate the equivalence adsorption data.

MATERIALS AND METHODS

The study was concocted in the Science and Research Branch of Islamic Azad University of Tehran, Iran in 2016.

Block copolymer surfactant Pluronic-123 with molecular weight (M_w=15800 g/mol) was purchased from Sigma-Aldrich. 3-chloropropyl trimethoxysilane was provided from Merck (Germany). PAMAM dendrimer (Generation Zero) was provided from the (Sigma-Aldrich, USA) and were selected as the adsorbents (Figure 1). Acid Red 266 was supplied by Dystar Co. (Figure 2). All used solvents and materials were analytical grade and purchased from Merck Company.

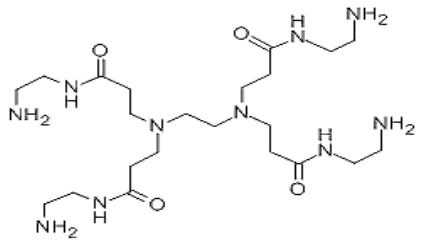

Figure 1. The chemical structure of dendrimers PAMAM (chemical formula $C_{22}H_{48}N_{10}O_4$, Mw = 517 g/mol, G_0)

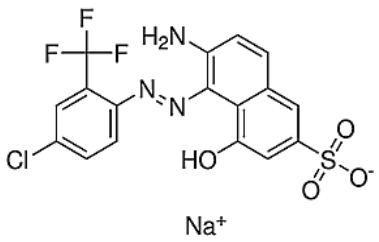

Figure 2. The chemical structure of Acid Red 266

Synthesis of SBA-15 and SBA-15-Den

SBA-15 was synthesized by the procedure modified [18], the amount of 4g block copolymer surfactant pluronic-123 was mixed with 125 cm^3 HCl (1.9 M) in aqueous media. The solution was homogenized at a temperature of 40 ºC and the monotonous and homogeneous solution was stirred by stirring consistently and continuously. Then, the amount of 8.58 g TEOS was added to the solution and was stirred for 20 h provided mixture was located about 24 h at 100 °C in a polyethylene container. The resulting solution was dried, filtered and calcined at 550 ºC for 10 h.

The amount of 10 g SBA-15 and 10 ml 3-chloropropyl trimethoxysilane was mixed with 15 ml toluene, and stirred for 15 min at room temperature by magnetic magnet and refluxed for 24 h. The resulting solution was cooled and filtered and orderly was washed by 30 ml toluene. The resulting product was dried under low pressure for 8 h at 100 °C to produce SBA-15-Cl (Figure 3) [19, 20].

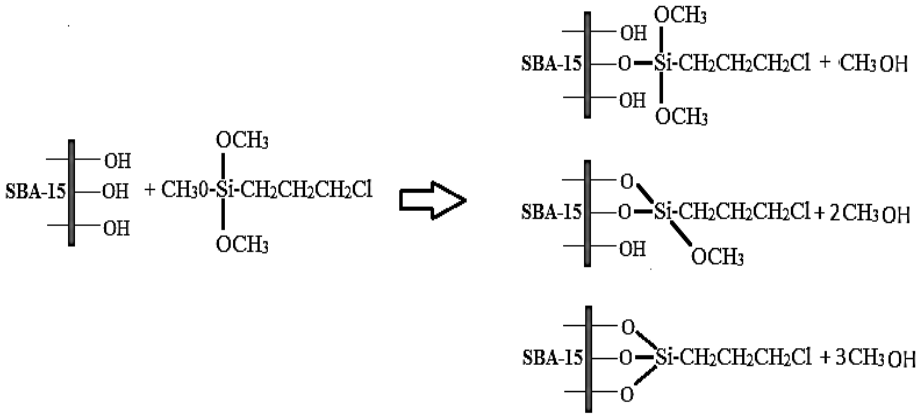

Figure 3. Scheme of SBA-15-Cl preparation

SBA-15-Cl was modified by PAMAM dendrimer by the addition of 5.16g of PAMAM dendrimer to 1g of chloro-mesoporous silica and dispersed in 50 ml of dry toluene. Then the mixture was refluxed at 70-80°C under stirring for 24 h, and then the synthesized material was filtered, washed with toluene, ethanol and diethyl ether, and then was dried for 8h at 70 °C to produce SBA-15-PAMAM (Figure 4) [21].

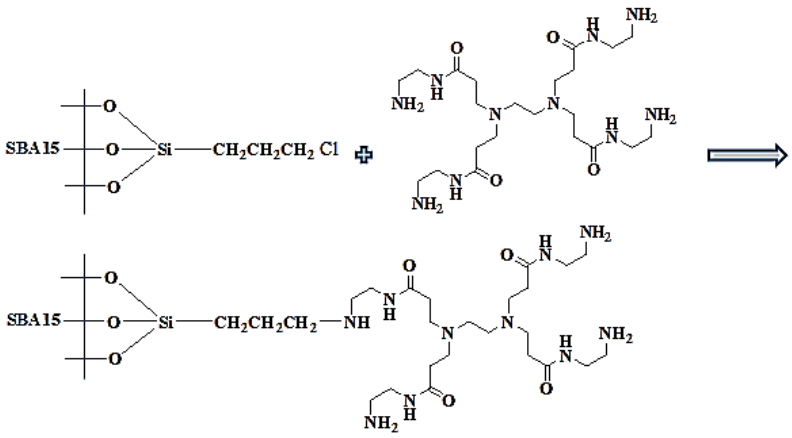

Figure 4. Scheme of the SBA-15/PAMAM preparation

Methods of Characterization

To better identify structural properties, identification tests were performed. Analytical techniques such as Fourier transform infrared (FT-IR**)** was registered with Perkin Elmer spectrum 400 in the range of 400-4000 cm^{-1} using KBr pellets, nitrogen physical adsorption isotherm (BET) and Pore Size and Volume Analysis (BJH) were carried out at 77.35 K with a PHS-1020 (PHS CHINA) apparatus**,** Field Emission Scanning Electron Microscopy (FE-SEM) observation was described with MIRAll TESCAN (Czech Republic).

Adsorption procedure

The dye adsorption quantification was performed by blending various amounts of SBA-15-PAMAM (0.01–0.1 g) for AR266 including of dye solution (40 ppm) at different pH_0 (2–12) in a shaker brooder (Heidolph). The pH of the solution was controlled by increasing a little value of H_2SO_4 or NaOH. At the termination of the adsorption tests, the solution specimens were centrifuged at 4000 rpm for 20 min and then the dye concentration was controlled applying Eq. (1). A spectrophotometer (UV-Vis) to control the concentration of AR266 in solution was used. The measurements in maximum wavelength (λ_{max}) of dye (AR266: 524nm) were carried out.

$$\text{Dye removal (\%)} = (C_0\text{-}C / C_0) \times 100 \qquad (1)$$

Where C_0 and C are respectively initial dye concentration (mg/l) and dye concentration (mg/l) at time t.

RESULTS AND DISCUSSION

Chemical characterization

The morphology of the SBA-15, SBA-15-Cl, and SBA-15-Den were studied by a scanning electron microscopy to confirm the high mesoscale order of the produced samples observed by FE-SEM. A regular and ordered structure with the relatively uniform size, which is in good agreement with SBA-15, can be observed in FE-SEM image (Figure 5a-5c). This can be seen on BET report (Table 1).

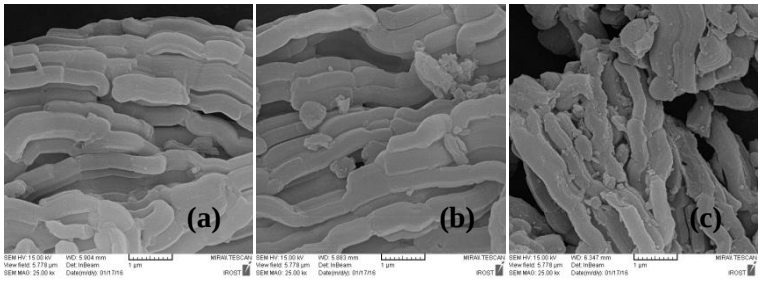

Figure 5. FESEM images of (a) SBA-15 (b) SBA-15-Cl (c) SBA-15-PAMAM

FTIR analysis used to determine the presence of functional groups in the chemical structure of SBA-15, SBA-15-Cl, and SBA-15-PAMAM (Figure 6). The conjunction of organic groups in the SBA-15 framework was stabilized by FT-IR spectra (Figure 6-(a)). A broad absorption band at 3450cm^{-1} for the unmodified SBA-15 sample is attributed to the –OH stretching vibrations of silanol groups and water molecules adsorbed. In three plots, the bands around 805 and 1091 cm^{-1} was seen, devoted to the typical symmetric and asymmetric stretching of Si-O-Si owing to condensed silica network. The broad peak around 3436, 3411 cm^{-1} was assigned to O-H stretching vibration of Si-O-H and HO-H of adsorbed water. In Figure 6-(b), the bands at 1434 and 1464 cm^{-1} dedicating to the -CH_2 bending vibration, while the peaks at 2851 and 2958 cm^{-1} were attributed to C-H stretching vibrations in the methylene groups of the aliphatic chain, showing the anchoring CPTMS on the silica surface [23]. The absorption band at 1556 cm^{-1} that obviously overlapped with bending vibration of adsorbed H_2O was related to N-H bending vibration of -NH_2 groups. Moreover, the peaks at 2923 and 3080 cm^{-1} were assigned to C-H stretching vibrations of the methylene groups. Therefore, the FT-IR results affirmed the conjunctions of functional groups on the SBA-15 silica surface [22, 23].

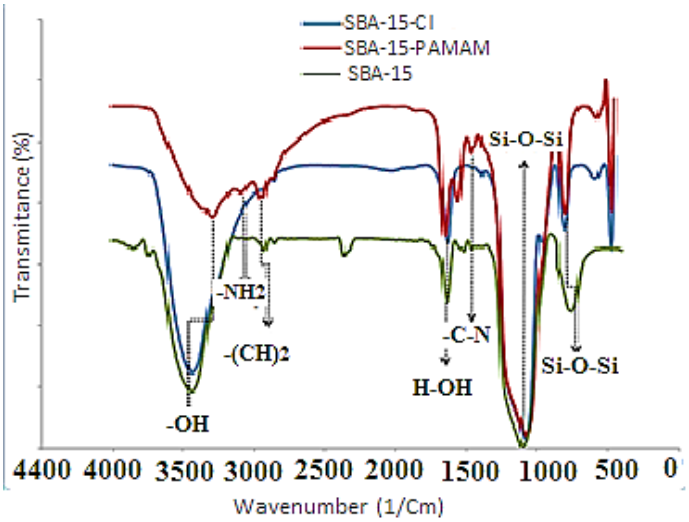

Figure 6. FTIR spectra of (a) SBA-15 (b) SBA-15-Cl (c) SBA-15-PAMAM

The N_2 adsorption–desorption isotherms were shown in Figure 7. In all materials, the "type IV" N_2 adsorption-desorption isotherms with "H_1-type" hysteresis loops, corresponded to condensation and evaporation steps, and were characteristic of periodic open-ended cylindrical mesoporous with narrow pore size distributions [25]. The mesoscopic structure of SBA-15 was preserved during the surface modification (Figure 7). Compared to SBA-15 material, SBA-15-Cl and SBA-15-PAMAM exhibited significantly lower BET surface area, pore volume, pore and higher wall thickness confirming that the surface modification takes place inside the silica Nano-channels (Table 1).

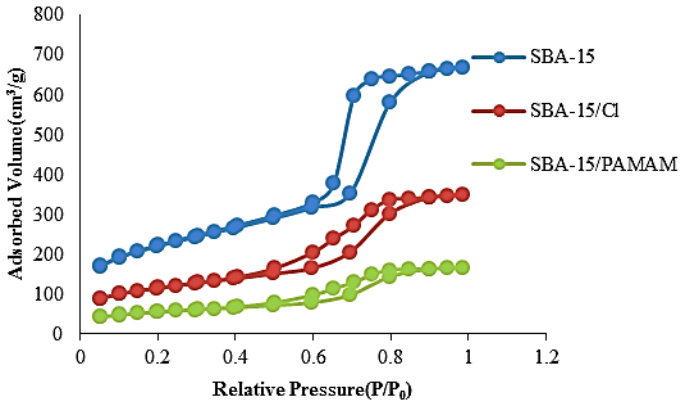

Figure 7. The N_2 adsorption/desorption isotherm of SBA-15, SBA-15-Cl, and SBA-15-PAMAM

Table 1. BJH results obtained for SBA-15, SBA-15-Cl, and SBA-15-Den

Sample	Specific surface area (BET) (m^2g^{-1})	Average pore diameter (BJH) (nm)	Pore Volume (BJH)(cm^3/g)
SBA-15	743.45	8.2	0.98
SBA-15-Cl	348.78	6.3	0.64
SBA-15-Den	165.94	4.1	0.36

Adsorption studies

Effect of initial pH

pH is an important factor on dye adsorption and it could affect the adsorbent characteristics and adsorbate specialization, mainly in instances of the dye adsorption [24, 25]. As seen in Figure 8, the decrease of initial pH was beneficial for increasing the dye removal, which several reasons can be ascribed to this tendency. Decreasing the pH value causes to rise in quantity of the amino groups and consequently, the adsorption behavior improves. Adsorption processes, mostly through the formation of covalent bonds between the Amin groups of dendrimer (PAMAM) and the anionic groups of dye molecules. The increase in the cationic amine groups is the important cause in the adsorption improvement of acid dyes [26, 27].

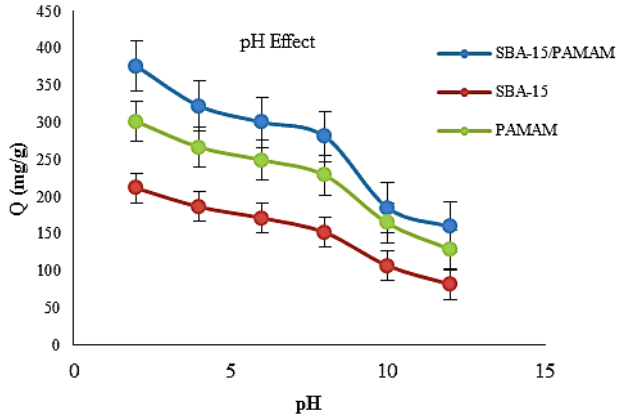

Figure 8. Effect of pH on dye removal (100ml of 40mg/l acidic dye, time=2h, T=25°C and the amount of adsorbent=10mg)

The number of cationic sites increases as the pH of the system decreases. Cationic sites on the SBA-15-PAMAM are preferred to the adsorption of acidic dyes because of the electrostatic adsorption. The general mechanism of adsorption of acidic dyes onto SBA-15-Den can be described in terms of Eq_s. (2) – (4):

$$SBA\text{-}15\text{-}Den\text{-}NH_2 \leftrightarrow SBA\text{-}15\text{-}Den\text{-}NH_3^+ \quad (2)$$

$$Dye\text{-}SO_3Na \leftrightarrow Dye\text{-}SO_3^- + Na^+ \quad (3)$$

$$SBA\text{-}15\text{-}Den\text{-}NH_3^+ + Dye\text{-}SO_3^- \leftrightarrow SBA\text{-}15\text{-}Den\text{-}NH_3^+ \quad (4)$$

Effect of adsorbent dosage

The maximum dye adsorption takes place at pH 2 (Figure 9). AB62 is a polar molecule ($R\text{-}SO_3^-$). SBA-15-PAMAM has primary amine groups at each branch end, affected by the pH of the solution. Therefore, the electrostatic attraction, as well as the organic properties and structure of dye molecules and dendrimer, could play a very important role in the dye adsorption on SBA-15-PAMAM. At pH 2, an electrostatic attraction exists between the positively charged surface of the dendrimer and the anionic dye. As the pH of the system increases, the number of positively charged sites decreases, which does not favor the adsorption of dye anions. The effective pH was 2 and it was used in further studies [28].

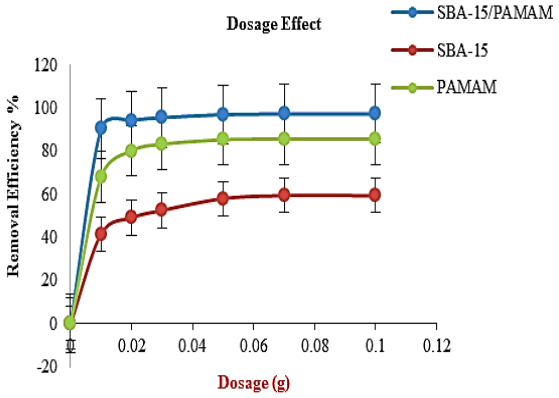

Figure 9. Effect of SBA-15, SBA-15-Cl, SBA-15-PAMAM adsorbent amount of dye adsorption (100ml of acidic dye solution with 40mg/l concentration at 25 °C and pH 2)

Effect of time and temperature

Studying the effect of temperature on adsorption was done at three various temperatures (25-35-45 °C). The obtained results were represented in Figure 10. At the initial stage of adsorption, dye removal has faster rate due to more active sites availability and then finally slower rate until the equilibrium is gotten at 60 min when adsorption sites become accomplished. The amount of adsorbate per unit mass of adsorbent at time *t* (mg/g), q_t enhances by decreasing temperature from 45 to 25 °C representing the exothermic nature of adsorption procedures [29, 30].

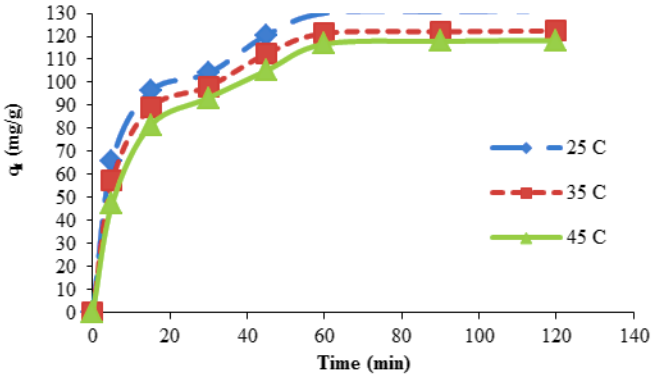

Figure 10. Effect of dye adsorption vs. contact time at various temperature 25, 35, 45°C (100ml acidic dye solution with 40mg/l concentration, 30 mg of SBA-15-PAMAM at pH 2)

Adsorption isotherms

The adsorption isotherm represents the relation among the mass of the dye absorbed at a specific temperature, pH, time and adsorbent dosage of the dye concentration. Four isotherms (Langmuir, Freundlich, Temkin and Dubbin Radushkevich isotherms) were studied. The Langmuir isotherm successfully applied for various adsorption processes might be applied to modify the dye adsorption onto SBA-15-PAMAM. The fundamental supposition of the Langmuir theory is that adsorption occurs at particular sites inside the adsorbent [31, 32]. The Langmuir isotherm model assumes monolayer adsorption on a surface with a limited number of similar sites, thus all sites are actively balanced and there is no interaction among the adsorbed molecules. The linear form of Langmuir equation is Eq. (5) [31, 32]:

$$C_e/q_e = 1/K_L Q_0 + C_e/Q_0 \qquad (5)$$

The amount of dye adsorbed on SBA-15-PAMAM at equilibrium, q_e, C_e, K_L and Q_0 (mg/g) are, the equilibrium concentration of dye solution (mg/l), dye concentration (mg/l), Langmuir constant (l/g) and the maximum adsorption capacity (mg/g), respectively. The amount of k_L and Q_0 values calculated from the slop and intercept of the plot of the c_e/q_e versus c_e (Figure 11). The K_L, Q_0, R_1^2 and R_L values are listed in Table 2.

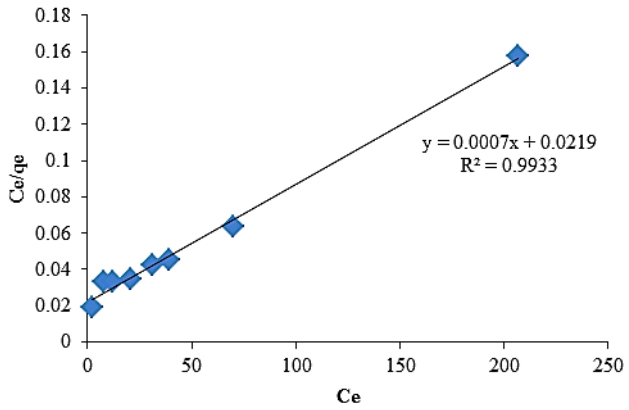

Figure 11. The Langmuir isotherm Plot for AR266 dye adsorption on SBA-15-PAMAM

The significant specifications the Langmuir isotherm may be represented by the dimensionless constant called equilibrium parameter R_L, identified by Eq. (6):

$$R_L = 1/1+K_LC_0 \quad (6)$$

The initial dye concentration is C_0 (mg/l) and R_L values show the type of isotherm to be irreversible (R_L = 0), favorable (0 < R_L < 1), linear (R_L = 1) or unfavorable (R_L > 1) [33].

As well as, isotherm data were tested with the Freundlich isotherm that can be reorganized to a linear form: Eq. (7) [13, 14 and 24]:

$$Logq_e = logK_F + 1/n\ logC_e \quad (7)$$

where *1/n* is adsorption intensity and K_F is adsorption capacity at unit concentration. *1/n* values indicate the type of isotherm to be invariable (*1/n* = 0), desirable (0 < *1/n* < 1) and undesirable (*1/n* > 1) [33].

The Freundlich explanation is an experimental equation for absorption on inharmonious surface with a non-uniform dispensation of adsorption heat over the surface and multilayer absorption. The amount of n and K_F values calculated from the slop and intercept of the plot of the lnq_e versus lnC_e (Figure 12). The K_F, n and R_2^2 values are listed in Table 2.

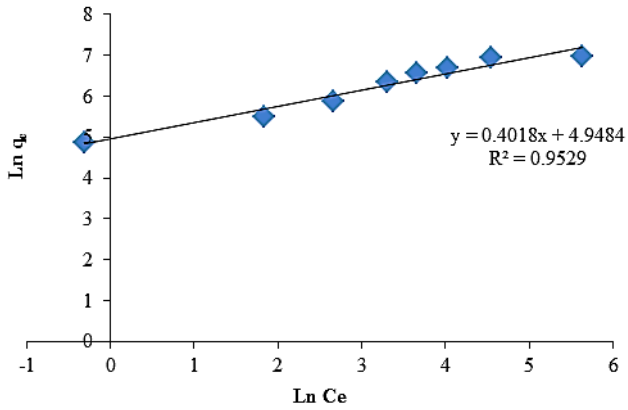

Figure 12. The Freundlich isotherm Plot for AR266 dye adsorption on SBA-15-PAMAM

The linearized Temkin isotherm absorption is shown as Eq. (8):

$$q_e = B_1 \ln K_T + B_1 \ln C_0 \quad (8)$$

Where Eq. (9)

$$B_1 = RT / b \quad (9)$$

Temkin isotherm encompasses a factor that is clearly extracting into the description adsorbing kind's adsorbent interactions [34]. A diagram of q_e versus in C_e provides the designation of the isotherm constants K_T and B_1 from the intercept and the slope, respectively.

Constant B_1 is referred to the heat of adsorption and K_T is the equilibrium binding constant (l/mol) correlating with the maximum binding energy. As well as, R, T, and b are the universal gas constant (8.314 j/mol k), the absolute temperature (K), and a constant, respectively. A plot of q_e versus lnC_e is used to determine the isotherm constants B_1 and K_T from the slope and intercept respectively (Figure 13).

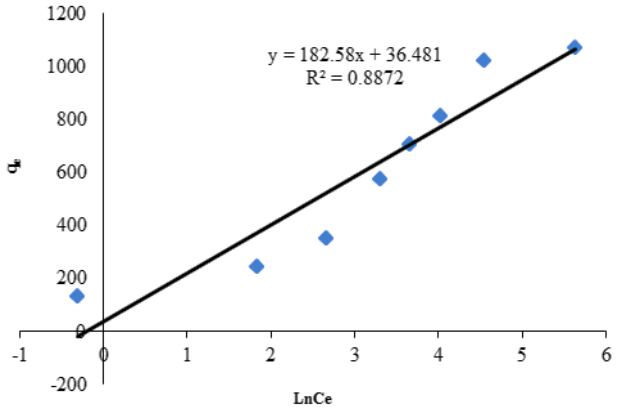

Figure 13. The Temkin isotherm Plot for AR266 dye adsorption on SBA-15-PAMAM

The D–R isotherm model was also used to study adsorption. The D–R isotherm can be applied to describe adsorption on both homogenous and heterogeneous surfaces [34]. A linear form of the D–R isotherm is:

$$\text{Ln } q_e = \ln q_m - \beta\varepsilon^2 \quad (10)$$

Where β, q_m and ε are a constant related to the mean free energy of adsorption (mol^2/kj^2), the theoretical saturation capacity and the Polanyi potential, respectively.

The Polanyi potential is given by RT ln(1 + 1/C$_e$)), where R (8.314 j/mol k) is the gas constant and T (K) is the absolute temperature (K).

To investigate the applicability of the D–R isotherm to adsorption of the dyes by SBA-15-PAMAM, in Figure 14, lnq_e was plotted against ε^2. D–R isotherm equation can be applied to obtain β values, which the mean energy of adsorption (E_a) can be calculated by use of Eq. (11) [34].

$$E_a = 2\beta^{-1/4} \quad (11)$$

Based on Eqs. (10) and (11), the isotherm constants, E_a and the correlation coefficient (R_4^2) were calculated and the values are shown in Table 2.

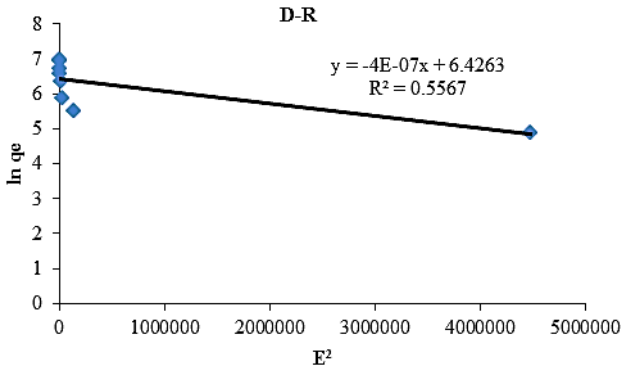

Figure 14. The Dubbin Radushkevich isotherm Plot for AR266 dye adsorption on SBA-15-

PAMAM

The K_L, Q_0, R_L, R_1^2 (the correlation coefficient for Langmuir isotherm), n, K_F, R_2^2 (the correlation coefficient for Freundlich isotherm) and B_1, K_T, and R_3^2 (the correlation coefficient for Temkin isotherm) and values of β, q_m and R_4^2 (the correlation coefficient for Dubbin Radushkevich isotherm) are listed in Table 2.

Table 2. Linearized isotherm coefficients for Acid Red 266 dye

Langmuir isotherm				Freundlich isotherm			Temkin isotherm			Dubbin radushkevich isotherm			
K_L	Q_0	R_1^2	R_L	K_F ((mg/g) (L/mg$^{1/n}$))	n	R_2^2	K_T (L/g)	B_1 (kj/mol)	R_3^2	β	q_m	R_4^2	E_a (Kj/mol)
0.048	1111.11	0.9914	0.339	140.95	2.489	0.9529	1.221	182.58	0.8872	17.87	617.88	0.5567	1.118

Adsorption and desorption studies

Desorption studies were carried out using NaOH (1M) solution. Results showed 18% drop in the adsorption capacity after first regeneration cycle (Figure 15). This decrease in adsorption capacity might be caused due to the decompositions or damages caused by alkaline solution to certain functional groups present on the surface of adsorbent (SBA-15/PAMAM). The decrease in the adsorption capacity was about 6% for the second and third cycle. The removal efficiency remains almost constant (76%) for the consecutive cycles (up to three cycles) showing that the adsorbent could be used repeatedly without any further losses in adsorption capacity.

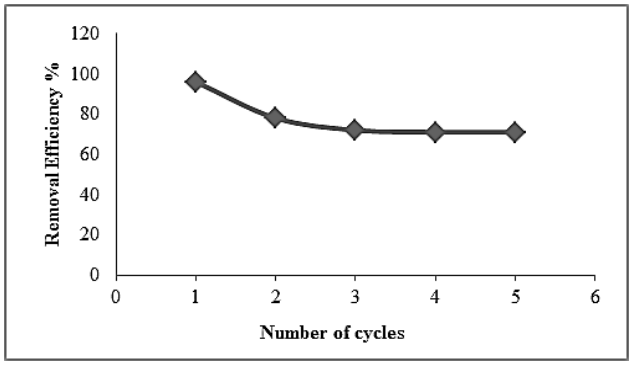

Figure 15. Regeneration studies of SBA-15/PAMAM. (Initial Concentration: 40 mg/l, contact time: 60 min, temperature: 25 °C, pH: 2, dosage: 0.3 g/l)

CONCLUSIONS

The interaction between SBA-15 and PAMAM dendrimer performed chemically in accordance with covalent chemical bonding. The decrease of pH was useful for raising dye removal from aqueous media. The maximum adsorption volume toward AR266 was 1111.11 mg/g. The adsorption isotherm study showed that the adsorption of AR266 corresponded well with Langmuir model. SBA-15-PAMAM has a good potential for removal of acid dye from aqueous media. The information obtained from Figure (11-14) and Table 2 represented that the Langmuir isotherm is the most suitable for adsorption of AR266 on SBA-15-PAMAM. Besides, the Langmuir isotherm presented superior fits than the Freundlich, Temkin and Dubbin Radushkevich isotherms. Therefore, the adsorption on the surface of SBA-15-PAMAM was a monolayer adsorption. The R_L values represented that adsorption was favorable for AR266. The studies have related to applying of Nano mesoporous adsorbent to remove acidic dyes from aqueous media.

Conflict of interest

The authors declare that there is no conflict of interest.

ACKNOWLEDGEMENTS

The authors wish to thank Science and Research Branch, Islamic Azad University and Qaemshahr Branch, Islamic Azad University for support of the project. The authors declare that there is no conflict of interest.

REFRENCES

1. Gupta V.K., Suhas, 2009. Application of low-cost adsorbents for dye removal – a review. J Environ Manage. 90, 2313-2342.

2. Piccin J.S., Vieira M.L.G., Goncalves J., Dotto G.L., Pinto L.A.A., 2009. Adsorption of FD and C Red No. 40 by chitosan: isotherms analysis. J Food Eng. 95, 16-20.

3. Dotto G.L., Pinto L.A.A., 2011, Adsorption of food dyes onto chitosan: optimization process and kinetic. Carbohydr Polym. 84, 231-238.

4. Salehi R., Arami M., Mahmoodi N.M., Bahrami H., Khorramfar S., 2010, Novel biocompatible Composite (chitosan–zinc oxide nanoparticle): preparation, characterization and dye adsorption properties. Colloids Surf B. 80, 86–93.

5. Kamble S.P., Mangrulkar P.A., Bansiwal A.K., Rayalu S.S., 2008. Adsorption of phenol and o-chloro phenol on surface altered fly ash based molecular sieves. Chem Eng J. 138, 73–83.

6. Zhao D., Huo Q., Feng J., Chmelka B.F., Stucky G.D., 1998. Nonionic tri block and star diblock copolymer and oligomeric surfactant syntheses of highly ordered, hydrothermally stable mesoporous silica structures. J Am Chem Soc. 120, 6024–6036.

7. Khodakov A.Y., Zholobenko V.L., Bechara R., Durand D., 2005. Impact of aqueous impregnation on the long-a georderingand mesoporous structure of cobalt containing MCM-41 and SBA-15 materials. Microporous Mesoporous Mater. 79, 29–39.

8. Zhao D.Y., Feng J.L., Huo Q.S., Melosh N., Fredrickson G.H., Chmelka B.F., Stucky G.D.,1998. Triblock copolymer syntheses of mesoporous silica with periodic 50 to 300 angestrom pores. Science. 279, 548–552.

9. Zhao D.Y., Huo Q.S., Feng J.L., Chmelka B.F., Stucky G.D.,1998. Nonionic triblock and star diblock copolymer and oligomeric surfactant syntheses of highly ordered, hydrothermally stable, mesoporous silica structures. J Am Chem Soc. 120, 6024–6036.

10. Tao Z.M., Xie Y.W., Goodisman J., Asefa T., 2010. Isomer-dependent adsorption and release of cis- and

trans-platin anticancer drugs by mesoporous silica nanoparticles. Langmuir. 26, 8914–8924.

11. Du G., Lim S.S., Pinault M., Wang C., Fang F., Pfefferle L., Haller G.L., 2008. Synthesis, characterization and catalytic performance of highly dispersed vanadium grafted SBA-15 catalyst. Catal J. 253, 74–90.

12. Ikemoto H., Chi Q.J., Ulstrup J., 2010. Stability and catalytic kinetics of horseradish peroxidase confined in nanoporous SBA-15. J Phys Chem C. 114, 16174–16180.

13. Prieto G., Martinez A., Murciano R., Arribas M.A., 2009. Cobalt supported on morphologically tailored SBA-15 mesostructures: the impact of pore lenghth on metal dispersion and catalytic activity in fischer-tropsch synthesis. Appl Catal A. 367, 146–156.

14. Badiei A., Goldooz H., Ziarani G.M., Abbasi A., 2011. One pot Synthesis of Functionalized SBA-15 by using an 8-Hydroxyquinoline-5-sulfonamide-modified Organo silane as Precursor. J Colloid Interface Sci. 357, 63- 69.

15. Bosman A.W., Janssen H.M., Meijer E.W., 1999. About dendimers: structure, physical properties, and applications. Chem Rev. 99, 1665-1688.

16. Bao C., Ran Lu M., Zhang T., Zhao Y., 2003. Preparation of Au nanoparticles in the presence of low generational poly (amid amine) dendrimer with surface hydroxyl groups. Mater Chem Phys. 81,160–165.

17. Weir M., Knecht M., Frenkel A., Crooks R., 2010. Structural analysis of Pd / Au dendrimer encapsulated bimetallic nanoparticles. Langmuir. 26, 1137–1146.

18. Boettcher S.W., Fan J., Tsung C.K., Shi Q., Stucky G.D., 2007. Harnessing the Sol–Gel Process for the Assembly of Non-Silicate Meso structured Oxide Materials. Acc Chem Res. 40, 784-792.

19. Matos J.R., Mercuri L.P., Kruk M., Jaroniec M., 2001. Toward the synthesis of extra-large pore MCM-41 analogues. Chem Mater. 13, 1726-1731.

20. Marino G., Bergamini M.F., Teixeira M.F.S., Cavalheiro E.T.G., 2003. Evaluation of carbon paste electrode modified with organofunctionalized amorphous silica in the cadmium determination in a differential pulse anodic stripping voltammetric procedure. Talanta. 59, 1021-1028.

21. Weber W.J., Morris J., Sanit C.J., 1963. Eng Div Am Soc Civil Eng. 89, 31- 46.

22. Badiei A., Goldooz H., Ziarani G.M., 2011. A novel method for preparation of 8-hydroxyquinoline functionalized mesoporous silica: Aluminum complexes and photoluminescence studies. Appl Surface Sci. 257, 4912-4918.

23. Badiei A., Goldooz H., Ziarani G.M., Abbasi A., 2011. One pot synthesis of functionalized SBA-15 by using an 8-hydroxyquinoline-5-sulfonamide-modified organosilane as precursor. J Colloid Interface Sci. 357, 63–69.

24. Kim S., Ida J., Guliants V.V., Lin J.Y.S., 2005. J Phys Chem B. 109, 6287–6293.

25. Tayebi H.A., Dalirandeh Z., Shokuhi Rad A., Mirabi A., Binaeian E., 2016. Synthesis of polyaniline/Fe_3O_4 magnetic nanoparticles for removal of reactive red 198 from textile waste water: kinetic, isotherm, and thermodynamic studies, Desalin. Water Treat. 7, 1-13.

26. Kyzas G.Z., Bikiaris D.N., 2008. Lazaridis N.K., Low-swelling chitosan derivatives as bio sorbents for basic dyes. Langmuir. 24, 4791–4799.

27. Crini G., Gimbert F., Robert C., Martel B., Adam O., Crini N.M., Giorgi F.D., Badot P.M., 2008. The removal of Basic Blue 3 from aqueous solutions by chitosan-based adsorbent: batch studies. J Hazard Mater. 153, 96–106.

28. Khorramfar S., Mahmoodi N.M., Arami M., Gharanjig K., 2010. Equilibrium and kinetic studies of the cationic dye removal capability of novel bio sorbent Tamarindus indicia from textile wastewater. Color Technol. 126, 261–268.

29. Alley E.R., Water Quality Control Handbook, 8th ed., McGraw Hill: New York, 2000. pp. 125–141.

30. Szyguła A., Guibal E., Ruiz M., Sastre A.M., 2008. The removal of sulphonated azo-dyes by coagulation with chitosan. Colloids Surf A. 330, 219–226.

31. Shafiabadi M., Dashti A., Tayebi H.A., 2016. Removal of Hg (II) from aqueous solution using polypyrrole/SBA-15 nanocomposite: Experimental and modeling. Syn Met. 212, 154-160.

32. Tayebi H.A., Yazdanshenas M.E., Rashidi A., Khajavi R., Montazer M., 2015. The isotherms, kinetics and thermodynamics of acid dye on nylon 6 with different amounts of titania and fiber cross sectional shape. J Eng Fiber Fab. 10, 97-108.

33. Langergren S., Svenska B.K., 1898. About the theory of so-called adsorption of soluble substances. Kungliga Svenska Vetenskapsakademiens Handlingar. 24, 1–39.

34. Mahmoodi N.M., Hayati B., Bahrami H., Arami M., 2011. Dye adsorption and desorption properties of Mentha pulegium in single and binary systems. J Appl Polym Sci. 122, 1489–1499.